Journal of Organometallic Chemistry 804 (2016) 18–25

Contents lists available at ScienceDirect

Journal of Organometallic Chemistry

journal homepage: www.elsevier.com/locate/jorganchem

Pentamethylcyclopentadienyltitanium aryl(pyridyl)amide complexes: Synthesis, characterization and catalytic performance for olefin polymerization

Qiang Zhang, Xin Tao**, Wei Gao, Tingting Song, Ying Mu*

State Key Laboratory for Supramolecular Structure and Materials, School of Chemistry, Jilin University, 2699 Qianjin Street, Changchun 130012, People's Republic of China

ARTICLE INFO

Article history:
Received 29 August 2015
Received in revised form
12 December 2015
Accepted 21 December 2015
Available online 24 December 2015

Keywords:
Atactic polypropylene
Half-titanocene complexes
Olefin polymerization
Polyethylene

ABSTRACT

A series of new half-sandwich pentamethylcyclopentadienyl titanium (IV) aryl(pyridyl)amide complexes, $Cp^*TiCl_2[N(Ar)(2\text{-}Py)]$ [Ar = 2,6-^{i}Pr$_2$Ph (**1**), 2,6-Et$_2$Ph (**2**), 2,6-Me$_2$Ph (**3**), 4-MePh (**4**)], have been synthesized from the reactions of Cp^*TiCl_3 with the lithium salts of the corresponding aryl(pyridyl)amido ligands in toluene. A byproduct with two aryl(pyridyl)amido ligands, $Cp^*TiCl[N(4\text{-}MePh)(2\text{-}Py)]_2$ (**5**) was also obtained from the synthetic reaction of complex **4** in a small amount. The new titanium complexes **1**–**4** were characterized by ^{1}H and ^{13}C NMR and elemental analyses. The molecular structures of complexes **1**, **2**, **4** and **5** were determined by single-crystal X-ray diffraction analysis. X-ray crystallographic analysis on complexes **1**, **2**, **4** demonstrates that these complexes possess a relatively crowded hepta-coordinating environment surrounding the central titanium atom. Upon activation with Al^{i}Bu$_3$ and $Ph_3CB(C_6F_5)_4$, complexes **1**–**4** exhibited moderate to high catalytic activity for ethylene and propylene polymerization, producing high molecular weight linear polyethylene and atactic polypropylene. It was found that complex **1** shows the highest catalytic activity for ethylene polymerization while complex **4** shows the highest catalytic activity for propylene polymerization among these complexes under similar conditions.

1. Introduction

Group 4 metallocene catalysts have attracted extensive interest in the past decades due to their unique properties and advantages as olefin polymerization catalysts [1–5]. Many research efforts have been focused on the development of new homogeneous metallocene catalysts for producing high performance polyolefin materials and understanding the relationship between the structure and catalytic property of a specific type of catalysts with respect to polymer chain composition and architecture [6–9]. Nonbridged half-titanocenes containing a variety of anionic ancillary ligands [5] have exhibited unique characteristics for the synthesis of new polymers that are not accessible by conventional Ziegler–Natta catalysts and "constrained geometry" titanium catalysts [6,8]. The synthesis of non-bridged half-metallocene complexes is generally simple, involving only one or two steps [5]. Furthermore, the structural modification in the steric and electronic environment of the ligand framework for this type of complexes is usually more facile than that for the bridged half-metallocene complexes [5]. The half-titanocene aryloxide catalyst systems, $Cp'TiCl_2(OAr)$ (Cp' = substituted cyclopentadienyl), were systematically studied by Nomura and co-workers and found to show good catalytic activity and efficient comonomer incorporation in olefin homo-/co-polymerization [10]. Similar non-bridged half-titanocene amide complexes, $Cp'TiCl_2(NR^1R^2)$ (R^1, R^2 = alkyl) [11] and anilide complexes $Cp'TiCl_2[N(2,6\text{-}R^1{}_2C_6H_3)R^2]$ (R^1 = Me, R^2 = SiMe$_3$ or Si^{t}BuMe$_2$) [12] have also been synthesized and investigated as catalysts for olefin polymerization. The reported results indicated that the half-titanocene anilide complexes exhibit extremely low catalytic activity for olefin polymerization with methylaluminoxane (MAO) as cocatalyst, although they are structurally similar to the non-bridged half-titanocene aryloxide complexes. Our previous research works indicated that appropriate structural modification on the anilido ligand of this type of complexes by changing the substituent R^2 on the N atom can improve their catalytic

* Corresponding author.
** Corresponding author.
E-mail address: ymu@jlu.edu.cn (Y. Mu).

http://dx.doi.org/10.1016/j.jorganchem.2015.12.029
0022-328X/

performance for olefin polymerization [13]. To further study the effect of the structure of the anilido ligand on the catalytic property of the non-bridged half-titanocene anilide complexes, we have recently synthesized a series of new half-titanocenes complexes with a chelated bidentate aryl(pyridyl)amido ligand, Cp*TiCl$_2$[-N(Ar)(2-Py)] [Ar = 2,6-^{i}Pr$_2$Ph (**1**), 2,6-Et$_2$Ph (**2**), 2,6-Me$_2$Ph (**3**), 4-MePh (**4**)], and found that they show moderate to high catalytic activity for ethylene and propylene polymerization, producing high molecular weight linear polyethylene and atactic polypropylene ($\overline{Mw}$ = 60–80 × 10^4 Da for aPP). Various metallocene [14–18] and non-metallocene complexes [19–22] of rare-earth and transition metals with different pyridylamido ligands have been previously reported. Of them, a number of half-hafnocene complexes with aryl(pyridyl)amido ligands were reported to exhibit moderate catalytic activity for ethylene polymerization [22]. To our knowledge, heretofore, only a few of catalyst systems have been reported for the synthesis of atactic polypropylene with weight-averaged molecular weight higher than 40 × 10^4 Da at room or above room temperatures [23]. Herein we report the synthesis and characterization of these new complexes as well as their catalytic performance in ethylene and propylene polymerization.

2. Results and discussion

2.1. Synthesis and characterization of the new complexes

The new half-titanocene aryl(pyridyl)amide complexes **1**–**4** were synthesized by the reactions of Cp*TiCl$_3$ with the lithium salts of corresponding aryl(pyridyl)amine compounds in 60–70% yields as shown in Scheme 1. The aryl(pyridyl)amines, Ar(2-Py)NH [Ar = 2,6-^{i}Pr$_2$Ph (H**L1**), 2,6-Et$_2$Ph (H**L2**), 2,6-Me$_2$Ph (H**L3**), 4-MePh (H**L4**)], were synthesized in about 90% yields through Pd-catalyzed coupling reactions of 2-bromopyridine with corresponding aniline derivatives following a literature procedure [24]. They were deprotonated by treatment with ^{n}BuLi in hexane to give their corresponding lithium salts, Ar(2-Py)NLi [Ar = 2,6-^{i}Pr$_2$Ph (Li**L1**), 2,6-Et$_2$Ph (Li**L2**), 2,6-Me$_2$Ph (Li**L3**), 4-MePh (Li**L4**)], which were isolated as white solids. The new half-titanocene aryl(pyridyl) amide complex **1** was synthesized in a yield of 67% from the reaction of Cp*TiCl$_3$ with 1 equiv of Li**L1** in toluene at 50 °C, while complexes **2**–**4** could not be obtained in reasonable yields under similar reaction conditions due probably to relatively weak nucleophilic reactivity of the lithium salts of these ligands Li**L2**-Li**L4**. Attempts to synthesize complexes **2**–**4** from the reactions of Cp*TiCl$_3$ with 1 equiv of lithium salts Li**L2**-Li**L4** in Et$_2$O and THF were not successful, too. Finally, complexes **2**–**4** were synthesized in 60–65% yields from reactions of Cp*TiCl$_3$ with 2 equiv of lithium salts Li**L2**-Li**L4** in toluene. From the reaction of Cp*TiCl$_3$ with 2 equiv of Li**L4** in toluene at room temperature, a by-product with two **L4** ligands, Cp*TiCl [N(4-MePh)(2-Py)]$_2$ (**5**), was also obtained in a small amount. Reactions at higher temperatures led to the formation of a mixture of complexes **4** and **5**, rendering the isolation of pure complex **4** difficult. In contrast, only monoamide complexes **1**–**3** could be obtained from the reactions of Cp*TiCl$_3$ with 2 equiv of Li**L1**- Li**L3**. It is apparent that the relatively large steric hindrance of **L1**-**L3** inhibits the formation of the diamide complexes in these reactions.

The new titanium complexes **1**–**4** were fully characterized by ^{1}H and ^{13}C NMR spectroscopy along with elemental analyses, and the structures of complexes **1**, **2**, **4** and **5** were confirmed by X-ray crystallography. The ^{1}H NMR spectrum of complex **1** shows two sets of doublets (1.28 and 0.93 ppm) for the methyl protons of the CH(C*H*$_3$)$_2$ group in ligand **L1** and the ^{13}C NMR spectrum of it shows two signals (25.6 and 23.8 ppm) for these two methyl carbons, indicating that the rotation of the 2,6-^{i}Pr$_2$C$_6$H$_3$ group around the N–C bond is restricted in complex **1**. These results were in agreement with the reported half-titanocence anilide complexes Cp'TiCl$_2$[N(2,6-^{i}Pr$_2$C$_6$H$_3$)Me] [13] but different from the half-titanocence aryloxide complexes Cp'TiCl$_2$[O-(2,6-^{i}Pr$_2$C$_6$H$_3$)] [10a]. In the latter case only one doublet for the methyl protons of the ^{i}Pr group was observed in their ^{1}H NMR spectra. Similar phenomenon was also observed for the resonances of the C*H*$_2$CH$_3$ protons in complex **2**, which show two sets of multiplets for the methylene protons. In comparison with the ^{1}H NMR spectrum of Cp*TiCl$_3$, the signals observed for the methyl protons of the CpMe$_5$ group in complexes **1**–**4** are shifted up field from 2.38 to 2.28 ppm (**1** and **2**), 2.29 ppm (**3**) and 2.17 ppm (**4**), respectively. The ^{1}H and ^{13}C NMR spectroscopic analyses of these complexes indicate that the ancillary aryl(pyridyl)amido ligands are attached to the titanium metal centers of these complexes.

2.2. Crystallographic analysis on complexes *1*, *2*, *4* and *5*

Molecular structures of complexes **1**, **2**, **4** and **5** were determined by single crystal X-ray diffraction analysis. The molecular structures of complexes **1**, **2** and **4** with the atom-numbering schemes are shown in Figs. 1–3, and selected bond lengths and angles of them are given in Table 1. The molecular structure together with selected bond lengths and angles of complex **5** are given in Fig. 4. As can be seen from their crystal structures, the coordination of the two nitrogen atoms in the aryl(pyridyl)amido ligand to the central metal of these complexes constructs a relatively crowded hepta-/octa-coordinating environment surrounding the central titanium atom. The Ti–N1(pyridyl) distances in complexes **1**, **2** and **4** [2.2528(19) Å for **1**, 2.205(2) Å for **2**, and 2.1809(19) Å for **4**] are obviously longer than the Ti–N2(amide) distances [2.0507(19) Å for **1**, 2.079(2) Å for **2**, and 2.0892(19) Å for **4**], demonstrating the coordination character of Ti–N(pyridyl) bond. The Ti–N(amido) distances in these complexes are longer than those observed in half-titanocence anilide complexes Cp*TiCl$_2$[N(2,6-^{i}Pr$_2$C$_6$H$_3$)Me] [13] and

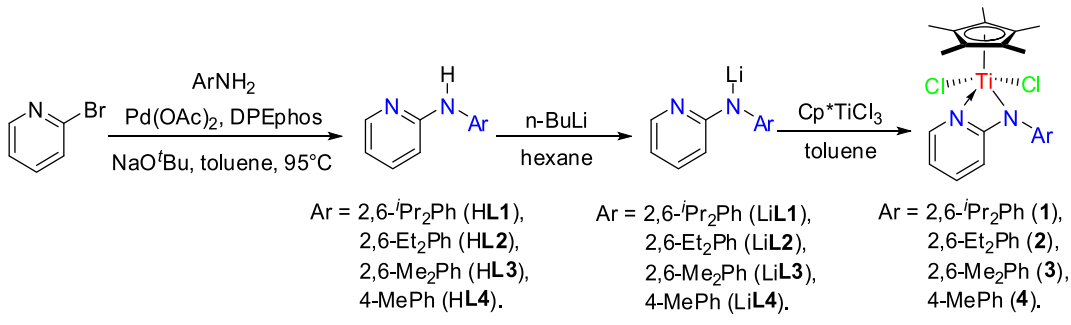

Scheme 1. The synthetic route for complexes **1**–**4**.

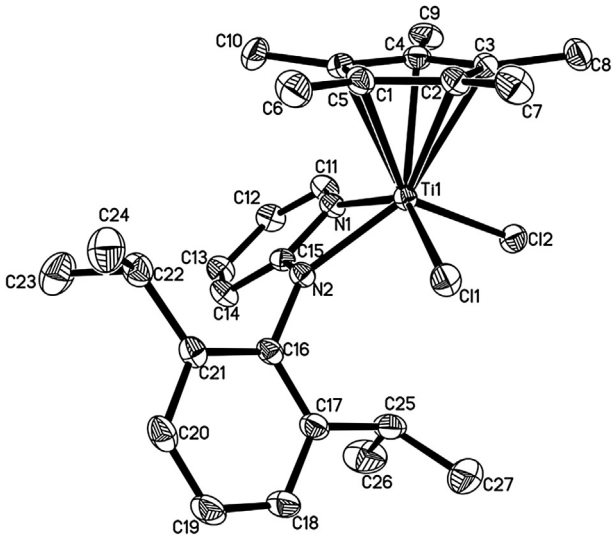

Fig. 1. Perspective view of complex **1** with thermal ellipsoids drawn at the 30% probability level. Hydrogens are omitted for clarity.

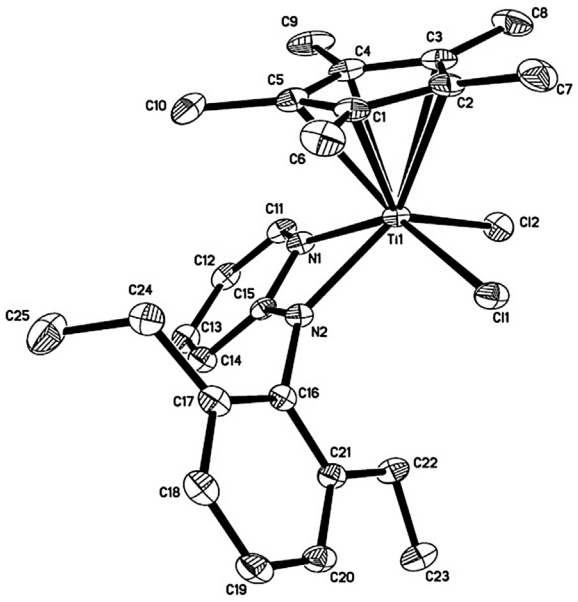

Fig. 2. Perspective view of complex **2** with thermal ellipsoids drawn at the 30% probability level. Hydrogens are omitted for clarity.

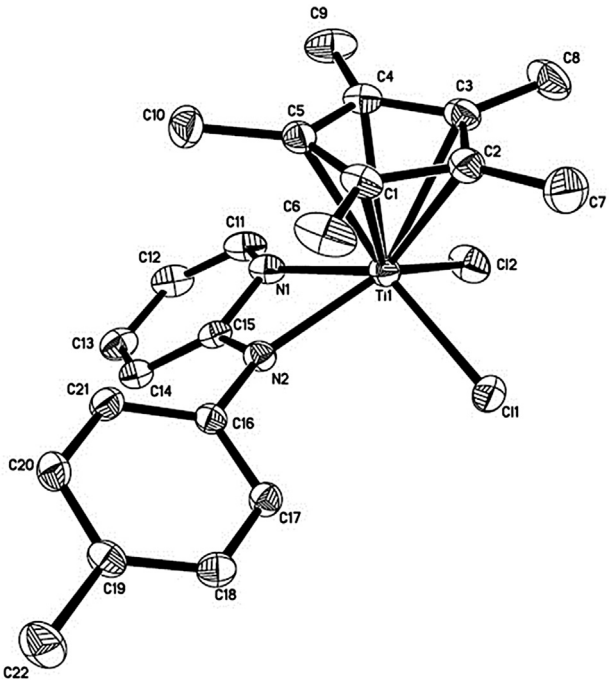

Fig. 3. Perspective view of complex **4** with thermal ellipsoids drawn at the 30% probability level. Hydrogens are omitted for clarity.

Table 1
Selected bond lengths (Å) and bond angles (deg) for complexes **1**, **2** and **4**.

	1	**2**	**4**
Ti(1)–Cp(cent)	2.076	2.070	2.046
Ti(1)–N(1)	2.2528(19)	2.205(2)	2.1809(19)
Ti(1)–N(2)	2.0507(19)	2.079(2)	2.0892(18)
Ti(1)–Cl(1)	2.3024(7)	2.3161(9)	2.3044(7)
Ti(1)–Cl(2)	2.2951(7)	2.2877(9)	2.3221(7)
Ti(1)–C(1)	2.364(2)	2.362(3)	2.352(2)
Ti(1)–C(2)	2.423(2)	2.401(3)	2.385(2)
Ti(1)–C(3)	2.450(2)	2.443(3)	2.393(2)
Ti(1)–C(4)	2.404(2)	2.404(3)	2.373(2)
Ti(1)–C(5)	2.354(2)	2.367(3)	2.364(2)
N(1)–C(15)	1.348(3)	1.348(4)	1.353(3)
N(2)–C(15)	1.361(3)	1.364(4)	1.358(3)
N(1)–Ti(1)–Cp(cent)	106.1	107.7	110.3
N(2)–Ti(1)–Cp(cent)	128.7	122.0	112.7
Cl(1)–Ti(1)–Cp(cent)	108.5	110.4	113.1
Cl(2)–Ti(1)–Cp(cent)	112.6	113.0	112.3
N(1)–Ti(1)–N(2)	61.37(7)	61.78(9)	61.78(7)
Cl(1)–Ti(1)–Cl(2)	95.05(3)	92.98(4)	91.35(3)

$Cp^*TiCl_2[N(2,6\text{-}Me_2C_6H_3)(SiMe_3)]$ [12], and the estimated value (2.02 Å) for Ti–N single bond according to Pauling's covalent radii [25]. It should be noted that, with the shortest Ti–N1 distance and longest Ti–N2 distance, the difference between the two Ti–N distances in complex **4** is the smallest among these complexes. On the other hand, the C15–N1 and C15–N2 bond distances [1.358(3) and 1.353(3) Å, respectively] in complex **4** are close to each other. These results are somewhat similar to the situation observed in the half-titanocene amidinate complex, $Cp^*TiCl_2[\eta^2\text{-}PhCH(Me)NCH(Me)NCH(Me)Ph]$ in which the amidinato ligand chelates to the Ti atom with Ti–N bond lengths of 2.114(2) and 2.157(2) Å, respectively [26]. In complex **5**, the Ti–N1 distance (2.247(3) Å) is obviously longer than the Ti–N2 distance (2.048(3) Å) as observed in complexes **1**, **2** and **4**. However, the Ti–N3 distance (2.191(3) Å) is much longer than the Ti–N(amido) distances in other complexes and the Ti–N4 bond distance (2.170(3) Å) is obviously shorter than the Ti–N(pyridyl) distances in other complexes. The Ti–Cl bond distances (2.288–2.322 Å) in complexes **1**, **2** and **4** are slightly longer than those (2.278–2.286 Å) observed in related anilido half-titanocence dichloride complexes [13], but shorter than the Ti–Cl bond distance in the crowded octa-coordinate complex **5**. The Ti–Cp(cent) distance in complex **5** (2.116 Å) is also longer than those in complexes **1** (2.076 Å), **2** (2.070 Å) and **4** (2.046 Å). The individual Ti–C(Cp) bond distances in these complexes range from 2.352 to 2.450 Å, with the Ti–C1 and Ti–C5 distances [2.364(2) and 2.354(2) Å for **1**, 2.362(3) and 2.367(3) Å for **2** and 2.352(2) and 2.364(2) Å for **4**] being obviously shorter than the remaining Ti–C(Cp) bond lengths (average 2.426, 2.416, and 2.384 Å for **1**, **2** and **4**, respectively), indicating that the central titanium atom is not located exactly below the centre of the Cp ring. The N1–Ti–N2

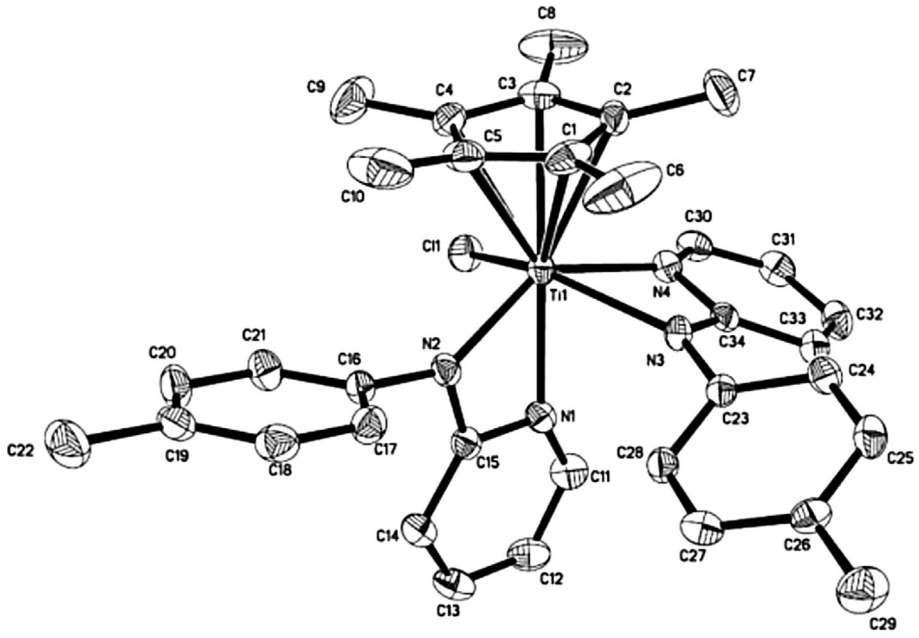

Fig. 4. Perspective view of complex **5** with thermal ellipsoids drawn at the 30% probability level. Hydrogens are omitted for clarity. Selected bond lengths (Å) and bond angles (deg): Ti(1)–Cp(cent) = 2.116, Ti(1)–N(1) = 2.247(3), Ti(1)–N(2) = 2.048(3), Ti(1)–N(3) = 2.191(3), Ti(1)–N(4) = 2.170(3), Ti(1)–Cl(1) = 2.4014(11), C(15)–N(1) = 1.341(4), C(15)–N(2) = 1.369(4), C(34)–N(3) = 1.337(4), C(34)–N(4) = 1.364(4), Cp(cent)–Ti(1)–Cl(1) = 104.9, Cp(cent)–Ti(1)–N(1) = 172.6, Cp(cent)–Ti(1)–N(2) = 110.0, Cp(cent)–Ti(1)–N(3) = 105.4, Cp(cent)–Ti(1)–N(4) = 107.6.

angles in these complexes are almost the same, being 61.37(7), 61.78(9) and 61.78(7)° for complexes **1**, **2** and **4**, respectively. The N(amide)–Ti–Cp(cent) angles in complexes **1**, **2** and **4** (128.74° for **1**, 122.0° for **2** and 112.7° for **4**) differ remarkably with the change in the size of the aryl(pyridyl)amido ligand in these complexes. The Cl1–Ti–Cl2 angles in these complexes [95.05(3)° for **1**, 92.98(4)° for **2** and 91.35(3)° for **4**] vary in the same trend as seen above for the N(amide)–Ti–Cp(cent) angles. These Cl–Ti–Cl angles are all much smaller than those observed in the half-titanocence anilide complexes $Cp^*TiCl_2[N(2,6\text{-}^iPr_2C_6H_3)Me]$ [104.91(12)°] and $Cp^*TiCl_2[N(2,6\text{-}Me_2C_6H_3)Me]$ [102.74(10)°] [13], indicating that these complexes possess a more crowded coordinating environment surrounding the central titanium atom in comparison to the half-titanocence anilide complexes. The above mentioned structural features may affect their catalytic performance by influencing the coordination of the olefin molecules to the titanium atoms and their insertion into the growing polymer chains, as well as the polymer chain termination process.

2.3. Ethylene polymerization

We have examined ethylene polymerization reactions using complexes **1**–**4** as precatalysts under different conditions and the results are summarized in Table 2. Upon activation with Al^iBu_3 and $Ph_3CB(C_6F_5)_4$, complexes **1**–**4** all exhibited moderate to high catalytic activity for the ethylene polymerization reaction. The catalytic activity of these complexes decreases in the order of **1** > **2** > **4** > **3** under similar conditions, demonstrating that the catalytic activity of these complexes is influenced by the nature of the aryl groups in their aryl(pyridyl)amido ligands. Similar change in catalytic activity has been previously observed with the half-titanocence anilide complexes [12,13]. As known for group 4 metallocene catalysts, electron-donating substituents on the ligands would stabilize the catalytically active cationic species during the polymerization and thus improve the catalytic activity of the catalyst; and bulky ligands would weaken the interaction between the catalytically active cationic species and the anionic cocatalyst and therefore could increase the catalytic activity of the catalyst [27,28]. The complex **4** showed a catalytic activity higher than the one observed for complex **3** due probably to that the steric hindrance of the aryl group in the amide ligand of complex **4** is much smaller than the one in complex **3** and therefore the coordination of the ethylene molecule to complex **4** becomes easier. The by-product **5** was also tested as a precatalyst for the ethylene polymerization reaction under similar conditions, and relatively low catalytic activity was observed. It is reasonable for the **5**/$Al^iBu_3/Ph_3CB(C_6F_5)_4$ system to show low catalytic activity since one of the two chelating aryl(pyridyl)amido

Table 2
Summary of ethylene polymerization catalyzed by **1**–**6**/$Al^iBu_3/Ph_3CB(C_6F_5)_4$ (**1**/MAO) systems.[a]

Entry	Catal	Al/Ti	Temp(°C)	Yield(g)	Activity[b]	M_η[c]($\times10^4$)	Tm[d](°C)
1	**1**	800	20	0.549	13176	108.2	139.2
2	**1**	800	35	0.750	18000	74.0	138.3
3	**1**	800	50	0.316	7584	56.9	140.0
4	**1**	600	35	0.286	6864	92.4	139.2
5	**1**	1000	35	0.468	11232	60.6	139.0
6[e]	**1**	800	35	0.432	10368	75.4	138.6
7[f]	**1**	800	35	0.342	8208	76.3	139.4
8[g]	**1**	2000	35	0.759	18216	54.7	136.7
9	**2**	800	35	0.700	16800	71.4	138.8
10	**3**	800	35	0.207	4968	56.5	139.5
11	**4**	800	35	0.375	9000	55.2	138.4
12	**5**	800	35	0.190	2280	55.8	138.7
13	**6**	800	35	0.392	9408	52.6	139.0
14	Cp^*TiCl_3	800	35	0.059	1416	32.1	138.4

[a] Polymerization conditions: solvent 80 ml of toluene; catalyst 0.5 μmol; B/Ti molar ratio 1.5; ethylene pressure 5 bar; time 5 min.
[b] Units of kg PE (mol Ti)$^{-1}$ h^{-1}.
[c] Measured in decahydronaphthalene at 135 °C.
[d] Determined by DSC at a heating rate of 10 °C min^{-1}.
[e] B/Ti molar ratio 1.
[f] B/Ti molar ratio 2.
[g] Activated with MAO.

ligands in complex **5** must be ripped off to form the catalytically active cationic species, which might take relatively long time and convert only partial of **5** to the active catalyst. When activated with MAO, complex **1** exhibited similar catalytic activity to the $Al^iBu_3/Ph_3CB(C_6F_5)_4$ activated catalyst system, but produced polyethylene with relatively low molecular weight. In comparison to the half-titanocence anilide analogues [12,13], these new half-titanocene complexes show obviously higher catalytic activities under similar conditions. To compare the catalytic performance of these new complexes with that of the known half-titanocene aryloxide and trichloride complexes, a typical complex $Cp^*TiCl_2[O(2,6\text{-}^iPr_2C_6H_3)]$ (**6**) was synthesized according to the literature procedure [10a] and the ethylene polymerization experiment with the **6**/$Al^iBu_3/Ph_3CB(C_6F_5)_4$ and $Cp^*TiCl_3/Al^iBu_3/Ph_3CB(C_6F_5)_4$ catalyst systems were conducted. It was found that, under the same conditions, complex **1** shows much higher catalytic activity and produces polyethylene with relatively high molecular weight in comparison with its aryloxide analogue **6** and Cp^*TiCl_3. The dependence of the catalytic activity of these new titanium catalyst systems on the Al/Ti molar ratio was examined and the maximal catalytic activity was observed with an Al/Ti molar ratio of 800. Ethylene polymerization experiments with these catalyst systems at different polymerization temperatures (20, 35 and 50 °C) were also carried out and the highest catalytic activity was obtained at 35 °C. The viscosity-averaged molecular weight (Mη) of the polyethylenes produced by these catalysts was measured in decahydronaphthalene at 135 °C. From these results, it can also be seen that the molecular weight of the resultant polyethylene is noticeably dependent on the structure of the catalyst. The molecular weight of the polyethylene changes with the catalyst in the order (**1** > **2** > **3** > **4**), due probably to that a relatively large aryl(pyridyl) amido ligand in the catalyst would lead to a relatively slow chain-transfer reaction [29]. The molecular weight of the polyethylene obtained from the **5**/$Al^iBu_3/Ph_3CB(C_6F_5)_4$ system is close to the one of the polyethylene from the **4**/$Al^iBu_3/Ph_3CB(C_6F_5)_4$ system, owing to that the catalytically active species is possibly the same in the two systems. The molecular weight of the obtained polyethylene was also influenced remarkably by the Al/Ti molar ratio and the polymerization temperature. As expected, the molecular weight of the produced polyethylene decreases with the increase in Al/Ti molar ratio and the elevation in polymerization temperature due to the acceleration of both the chain transfer reaction to alkylaluminum and the β-hydride elimination reaction. In addition, the melting temperatures of the resultant polyethylenes (138.3–140.0 °C) are in the normal range for linear polyethylene. ^{13}C NMR spectroscopic analysis on typical polyethylene samples (see Supplementary Material) confirms the linear structure of the obtained polyethylene. By the way, it was found that the **1**–**4**/$Al^iBu_3/Ph_3CB(C_6F_5)_4$ systems couldn't catalyze the copolymerization of ethylene with long chain α–olefins, such as 1-hexene and 1-octene, which is quite different from the similar half-titanocence anilide and aryloxide catalyst systems [10,13].

2.4. Propylene polymerization

Propylene polymerization reactions with the **1**–**4**/$Al^iBu_3/Ph_3CB(C_6F_5)_4$ catalyst systems were also investigated and the experimental results are summarized in Table 3. Upon activation with Al^iBu_3 and $Ph_3CB(C_6F_5)_4$, complexes **1**–**4** all exhibited excellent catalytic activity (up to 5058 kg PP (mol Ti)$^{-1}$ h^{-1}) for the propylene polymerization reaction and produced polypropylenes as elastomeric solid materials. In contrast to the case of ethylene polymerization reaction, the catalytic activity of these complexes for the propylene polymerization reaction decreases in the order of **4** > **3** > **2** > **1** under similar conditions. It seems that a relatively large aryl(pyridyl)amido ligand in the catalyst would slow down the coordination of the bulkier propylene molecule to the metal center of the catalyst and insertion into the growing polymer chain [28b]. ^{13}C NMR analysis on typical polypropylene samples (see Supplementary Material) indicates that atactic polypropylene was formed from these catalyst systems [30]. It was expected for these catalyst systems to produce isotactic or atactic polypropylene based on their flexible C_1- or C_s-symmetric structural feature [23]. ^1H NMR spectra of typical polypropylene samples show no resonance for olefinic termination groups (see Supplementary Material), demonstrating that the main polymer chain termination step of the polymerization reaction is not the β–hydride elimination process [28b]. GPC analysis indicates that the obtained polypropylene samples possess high molecular weight and narrow molecular weight distributions (PDI range from 1.98 to 3.32). From a structural point of view, the crowded hepta-coordinating environment around the central metals of these catalysts would inhibit the chain transfer and β-hydride elimination reactions and lead to the formation of the high molecular weight atactic polypropylene. It can be seen from the data that the molecular weight of the polypropylenes is evidently dependent on the structure of the catalyst. Both chain growth and chain transfer reactions can be slowed down on a bulky catalyst. However, the effect on the two reactions may be quite different depending on the structure of the catalyst. In the bulkiest catalyst **1** system, the chain growth reaction might be slowed down more remarkably in contrast to the chain transfer reaction. The low catalytic activities of catalyst **1** system have demonstrated the slow chain growth reaction. In the least bulky catalyst **4** system, the chain growth reaction is much fast and the ratio of the chain growth rate to the chain transfer rate is larger than the one in catalyst **1** system. Therefore the highest molecular weight polypropylene was produced by the least bulky catalyst **4** while the lowest molecular weight polypropylene was produced by the bulkiest catalyst **1**. The **5**/$Al^iBu_3/Ph_3CB(C_6F_5)_4$ catalyst system was also examined for the propylene polymerization reaction with low catalytic activity being observed and high molecular weight atactic polypropylene similar to the one produced by the **4**/$Al^iBu_3/Ph_3CB(C_6F_5)_4$ catalyst system being obtained. These results further demonstrate that the catalytically active species in the two systems may be the same.

Table 3
Summary of propylene polymerization catalyzed by **1**–**5**/$Al^iBu_3/Ph_3CB(C_6F_5)_4$ systems.[a]

Entry	Catal	Al/Ti	Yield(g)	Activity[b]	$\overline{Mw}$ [c] (×10^4)	$\overline{Mw}/\overline{Mn}$[c]
1	**1**	300	0.152	912	3.50	2.77
2	**1**	200	0.246	1476	6.68	3.32
3	**1**	100	trace	–	–	–
4	**2**	200	0.402	2412	65.60	2.36
5	**3**	200	0.624	3744	68.78	2.47
6	**4**	200	0.843	5058	81.12	1.98
7	**5**	200	0.054	324	83.97	1.91

[a] Polymerization conditions: solvent 80 ml of toluene; catalyst 2 μmol; B/Ti molar ratio 1.5; propylene pressure 5 bar; time 5 min; temperature 35 °C.
[b] Units of kg PP (mol Ti)$^{-1}$ h^{-1}.
[c] Determined by GPC analysis in THF at 40 °C against polystyrene standard.

3. Conclusions

A series of new half-sandwich pentamethylcyclopentadienyl titanium (IV) aryl(pyridyl)amide complexes, $Cp^*TiCl_2[N(Ar)(2\text{-}Py)]$ (**1**–**4**) have been synthesized from the reactions of Cp^*TiCl_3 with the lithium salts of the corresponding aryl(pyridyl)amido ligands and characterized by ^1H and ^{13}C NMR and elemental analyses. X-ray crystallographic analysis on complexes **1**, **2** and **4** demonstrates that

these complexes possess a relatively crowded hepta-coordinating environment around their central titanium atoms. Upon activation with Al^iBu_3 and $Ph_3CB(C_6F_5)_4$, complexes **1**–**4** all exhibit excellent catalytic activity for ethylene and propylene polymerization, producing high molecular weight linear polyethylene and high molecular weight atactic polypropylene. Among these complexes, the bulkiest complex **1** shows the highest catalytic activity for ethylene polymerization while the least bulky complex **4** shows the highest catalytic activity for propylene polymerization under similar conditions.

4. Experimental section

4.1. General methods

All manipulations involving air- and/or moisture-sensitive compounds were carried out under nitrogen atmosphere (ultra-high purity) using either standard Schlenk or glove box techniques. Toluene, diethyl ether, THF, *n*-pentane and *n*-hexane were distilled under nitrogen in the presence of sodium and benzophenone. CH_2Cl_2 was dried by distilling over calcium hydride before use. Cp^*TiCl_3 [31] and $Ph_3CB(C_6F_5)_4$ [32] were prepared according to literature procedures. Polymerization grade ethylene and propylene was further purified by passage through columns of 5 Å molecular sieves and MnO. Al^iBu_3, *n*-BuLi, $TiCl_4$, 2-bromopyridine, $Pd(OAc)_2$, NaO^tBu, DPEphos, 2,6-dimethylaniline, 2,6-diethylaniline, 2,6-diisopropylaniline and 4-methylaniline were purchased from Aldrich or Acros. ^1H and ^{13}C NMR spectra were recorded using a Varian Mercury-300 or a Bruker Avance III-400 NMR spectrometer. ^{13}C NMR spectra of the polymers were recorded on a Bruker Avance III-400 NMR spectrometer at 135 °C with *o*-$C_6D_4Cl_2$ as the solvent. The viscosity-averaged molecular weight ($M\eta$) of the polyethylene samples was measured in decahydronaphthalene at 135 °C by a Ubbelohde viscometer according to the following equation: $[\eta] = 6.77 \times 10^{-4}\ M\eta^{0.67}$. The molecular weights and molecular weight distributions of the atactic polypropylene samples were determined at 40 °C by gel permeation chromatography equipped with a Waters 515 HPLC pump, four columns (HMW 7 THF, HMW 6E THF × 2, HMW 2 THF) and a Waters 2414 refractive index detector. THF was used as the eluent at a flow rate of 1.00 mL/min against polystyrene standards with Mark-Houwink corrections. The melting points of the polyethylenes were measured by differential scanning calorimetry (DSC) on a NETZSCH DSC 204 at a heating/cooling rate of 10 °C/min from 35 to 160 °C and the data from the second heating scan were used.

4.2. Synthesis of 2,6-$^iPr_2C_6H_3$(2-Py)NH (H**L1**)

$Pd(OAc)_2$ (22.4 mg, 0.10 mmol), NaO^tBu (1.15 g, 12.0 mmol) and DPEphos (80.8 mg, 1.15 mmol) were mixed with a solution of 2-bromopyridine (1.58 g, 10.0 mmol) and 2,6-diisopropylaniline (1.77 g, 10.0 mmol) in toluene (20 mL) under nitrogen atmosphere. This suspension was stirred at 95 °C overnight. The reaction mixture was cooled to room temperature and quenched with water (40 mL). The mixture was extracted with ethyl acetate (3 × 20 mL). The combined organic phases were dried with anhydrous $MgSO_4$, filtered and concentrated by distillation under reduced pressure to give an solid crude product and the solid product was recrystallized from absolute ethanol to yield the pure product H**L1** (2.33 g, 9.16 mmol, 91.6%) as a white powder. ^1H NMR ($CDCl_3$, 300 MHz, 298 K) δ 8.13 (dd, J = 5.1, 1.9 Hz, 1H, Py*H*), 7.39–7.20 (m, 4H, Py*H*, Ph*H*), 6.62 (m, 1H, Py*H*), 6.15 (br, 1H, N*H*), 5.99 (d, J = 8.4 Hz, 1H, Py*H*), 3.20 (m, J = 6.9 Hz, 2H, C*H*$(CH_3)_2$), 1.14 (d, J = 6.9 Hz, 12H, CH(C*H*$_3)_2$) ppm.

4.3. Synthesis of 2,6-$Et_2C_6H_3$(2-Py)NH (H**L2**)

Compound H**L2** was synthesized in the same manner as described for H**L1** with 2-bromopyridine (1.58 g, 10.0 mmol) and 2,6-diethylaniline (1.49 g, 10.0 mmol) as the starting materials. Pure product (2.04 g, 9.01 mmol, 90.1%) was obtained as a white crystalline material. ^1H NMR ($CDCl_3$, 300 MHz, 298 K): δ 8.13 (d, J = 5 Hz, 1H, Py*H*), 7.35 (t, J = 8 Hz, 1H, Py*H*), 7.25 (d, J = 7 Hz, 1H, Ph*H*), 7.19 (d, J = 7 Hz, 2H, Ph*H*), 6.62 (t, J = 6 Hz, 1H, Py*H*), 6.35 (br, 1H, N*H*), 6.00 (d, J = 8 Hz, 1H, Py*H*), 2.61 (q, J = 7 Hz, 4H, C*H*$_2$CH$_3$), 1.15 (t, J = 7 Hz, 6H, CH$_2$C*H*$_3$) ppm.

4.4. Synthesis of 2,6-$Me_2C_6H_3$(2-Py)NH (H**L3**)

Compound H**L3** was synthesized in the same manner as described for H**L1** with 2-bromopyridine (1.58 g, 10.0 mmol) and 2,6-dimethylaniline (1.21 g, 10.0 mmol) as the starting materials. Pure product (1.83 g, 9.23 mmol, 92.3%) was obtained as a white crystalline material. ^1H NMR ($CDCl_3$, 300 MHz, 298 K) δ 8.14 (d, J = 5.1 Hz, 1H, Py*H*), 7.44–7.32 (m, 1H, Py*H*), 7.14 (s, 3H, Ph*H*), 6.69–6.60 (m, 1H, Py*H*), 6.18 (br, 1H, N*H*), 6.02 (d, J = 8.4 Hz, 1H, Py*H*), 2.23 (s, 6H, ArC*H*$_3$) ppm.

4.5. Synthesis of 4-MeC_6H_3(2-Py)NH (H**L4**)

Compound H**L4** was synthesized in the same manner as described for H**L1** with 2-bromopyridine (1.58 g, 10.0 mmol) and 4-methylaniline (1.07 g, 10.0 mmol) as the starting materials. Pure product (1.67 g, 9.09 mmol, 90.9%) was obtained as a white crystalline material. ^1H NMR ($CDCl_3$, 400 MHz, 298 K) δ 8.17 (ddd, J = 5.0, 1.9, 0.9 Hz, 1H, Py*H*), 7.46 (ddd, J = 8.5, 7.2, 1.9 Hz, 1H, Py*H*), 7.23–7.12 (m, 4H, Ph*H*), 6.81 (dt, J = 8.4, 0.9 Hz, 1H, Py*H*), 6.69 (ddd, J = 7.2, 5.0, 0.9 Hz, 1H Py*H*), 2.33 (s, 3H, PhC*H*$_3$) ppm.

4.6. Synthesis of complex ***1***

A solution of ^{n}BuLi (1.60 M in *n*-hexane, 3.9 mL, 6.25 mmol) was slowly added to a solution of 2,6-$^iPr_2C_6H_3$(2-Py)NH (1.59 g, 6.25 mmol) in *n*-hexane (20 mL) at −20 °C, during which period a large amount of white precipitate formed. The reaction mixture was allowed to warm to room temperature and stirred for 5 h. The resultant precipitate was collected on a frit, washed with cold *n*-hexane (2 × 10 mL) and dried under vacuum to give 2,6-$^iPr_2C_6H_3$(2-Py)NLi as a white solid. Then Cp^*TiCl_3 (1.45 g, 5.00 mmol) and 2,6-$^iPr_2C_6H_3$(2-Py)NLi (1.30 g, 5.00 mmol) were mixed in toluene (15 mL) at −78 °C. The reaction mixture was allowed to warm to room temperature first and then stirred at 50 °C overnight. The precipitate was filtered off and the filtrate was concentrated to leave a dark brown residue. Recrystallization from CH_2Cl_2/*n*-hexane gave pure product **1** (1.69 g, 3.33 mmol, 66.7%) as reddish brown crystals. Anal. Calcd. for $C_{27}H_{36}Cl_2N_2Ti$ (507.36): C, 63.92; H, 7.15; N, 5.52. Found: C, 63.66; H, 7.09; N, 5.67. ^1H NMR ($CDCl_3$, 300 MHz, 298 K): δ 8.09 (m, 1H, Py*H*), 7.32–7.24 (m, 1H, Py*H*), 7.17–7.10 (m, 3H, Ph*H*), 6.54 (m, 1H, Py*H*), 5.55–5.50 (m, 1H, Py*H*), 3.25–3.15 (m, 2H, C*H*$(CH_3)_2$), 2.29 (s, 15H, CpC*H*$_3$), 1.28 (d, J = 6.8 Hz, 6H, CH(C*H*$_3)_2$), 0.93 (d, J = 6.8 Hz, 6H CH(C*H*$_3)_2$) ppm. ^{13}C NMR ($CDCl_3$, 75 MHz, 298 K): δ 167.1, 147.3, 144.0, 143.2, 140.9, 134.1, 126.5, 123.9, 112.6, 105.0(Ar*C*, Py*C*), 28.0 (*C*H$(CH_3)_2$), 25.6 (CH(*C*H$_3)_2$), 23.8 (CH(*C*H$_3)_2$), 14.2 (Cp*C*H$_3$) ppm.

4.7. Synthesis of complex ***2***

A solution of ^{n}BuLi (1.60 M in *n*-hexane, 7.9 mL, 12.5 mmol) was slowly added to a solution of 2,6-$Et_2C_6H_3$(2-Py)NH (2.83 g, 12.5 mmol) in *n*-hexane (20 mL) at −20 °C, during which period a

Table 4
Details of the crystal data, data collections, and structure refinements for complexes **1**, **2**, **4**, **5**.

	1	**2**	**4**	**5**
Formula	$C_{27}H_{36}Cl_2N_2Ti$	$C_{25}H_{32}Cl_2N_2Ti$	$C_{22}H_{26}Cl_2N_2Ti$	$C_{34}H_{37}ClN_4Ti$
Formula weight (g mol^{-1})	507.38	479.33	437.25	585.03
Crystal system	Triclinic	Triclinic	Monoclinic	Monoclinic
Space group	P-1	P-1	P2(1)/c	C2/c
a (Å)	10.4775(6)	8.2562(12)	12.5631(8)	37.646(3)
b (Å)	10.9153(6)	8.6298(12)	9.2521(6)	9.0705(6)
c (Å)	12.4145(7)	18.433(3)	18.9574(12)	17.8978(12)
α (deg)	84.7360(10)	97.415(2)	90	90
β (deg)	83.8360(10)	98.059(2)	104.9510(10)	92.5620(10)
γ (deg)	70.9360(10)	113.304(2)	90	90
V (Å^3)	1331.73(13)	1169.4(3)	2128.9(2)	6105.4(7)
Z	2	2	4	8
ρ, calcd, (g cm^{-3})	1.265	1.361	1.364	1.273
Abs coeff/mm^{-1}	0.539	0.609	0.662	0.397
θ range (deg)	1.65 − 26.03	2.28 − 26.08	1.68 − 25.05	2.17−25.04
R(int)	0.0152	0.0251	0.0258	0.0584
Data/restraints/parameters	5131/0/298	4489/0/278	3750/0/250	5386/0/368
GOF	1.037	1.122	1.057	1.136
R1, Rw [I > 2sigma(I)]	0.0438, 0.1066	0.0558, 0.1417	0.0370, 0.0955	0.0685, 0.1384
R1, Rw (all data)	0.0535, 0.1135	0.0627, 0.1476	0.0439, 0.1010	0.0954, 0.1504
Max(min) diff peak (e Å^{-3})	0.340, −0.193	0.957, −0.445	0.310, −0.215	0.380, −0.265

large amount of white precipitate formed. The reaction mixture was allowed to warm to room temperature and stirred for 5 h. The resultant precipitate was collected on a frit, washed with cold *n*-hexane (2 × 10 mL) and dried under vacuum to give 2,6-$Et_2C_6H_3$(2-Py)NLi as a white solid. Then Cp*$TiCl_3$ (1.45 g, 5 mmol) and 2,6-$Et_2C_6H_3$(2-Py)NLi (2.32 g, 10 mmol) were mixed in toluene (15 mL) at −78 °C. The reaction mixture was allowed to warm to room temperature and stirred for 1 h. The precipitate was filtered off and the solvent was removed under reduce pressure to leave a dark brown residue. Recrystallization from CH_2Cl_2/*n*-hexane gave pure product **2** (1.58 g, 3.29 mmol, 65.8%) as reddish brown crystals. Anal. Calcd. for $C_{25}H_{32}Cl_2N_2Ti$ (479.31): C, 62.65; H, 6.73; N, 5.84. Found: C, 62.32; H, 6.68; N, 5.92. ^{1}H NMR ($CDCl_3$, 400 MHz, 298 K) δ 8.09 (d, J = 5.3 Hz, 1H, Py*H*), 7.38−7.23 (m, 3H, Ph*H*), 7.23−7.16 (d, J = 7.6 Hz, 1H, Py*H*), 6.55 (t, J = 6.3 Hz, 1H, Py*H*), 5.51 (d, J = 8.4 Hz, 1H, Py*H*), 3.03−2.67 (m, 2H, CH_2CH$_3$), 2.67−2.44 (m, 2H, CH_2CH$_3$), 2.23(s, 15H, CpCH_3), 1.12 (t, 6H, CH$_2$CH_3). ^{13}C NMR ($CDCl_3$, 100 MHz, 298 K) δ 165.8, 148.1, 143.4, 141.3, 139.2, 134.2, 126.1, 125.9, 112.6, 104.0(Ar*C*, Py*C*), 24.4 (CH_2CH$_3$), 14.9 (CH$_2$CH_3), 14.2 (CpCH_3) ppm.

4.8. Synthesis of complex *3*

Complex **3** was synthesized in the same manner as described for complex **2**. Pure **3** (yield 64.6%) was obtained as reddish brown crystals by recrystallization from CH_2Cl_2/*n*-hexane. Anal. Calcd. for $C_{23}H_{28}Cl_2N_2Ti$ (451.25): C, 61.22; H, 6.25; N, 6.21. Found: C, 61.48; H, 6.29; N, 6.32. ^{1}H NMR ($CDCl_3$, 300 MHz, 298 K): δ 8.09 (d, J = 4.6 Hz, 1H, Py*H*), 7.32 (t, J = 7.1 Hz, 1H, Py*H*), 7.04 (m, 4H, Ph*H*), 6.59−6.53 (m, 1H, Py*H*), 5.48 (d, J = 8.4 Hz, 1H, Py*H*), 2.29 (s, 15H, CpCH_3), 2.21 (s, 6H, PhCH_3) ppm. ^{13}CNMR ($CDCl_3$, 75 MHz, 298 K): δ 149.5, 143.6, 141.6, 134.2, 133.7, 128.5, 125.6, 112.7, 103.5(Ar*C*, Py*C*), 19.5 (ArCH_3), 14.3 (CpCH_3) ppm.

4.9. Synthesis of complex *4*

Complex **4** was synthesized in the same manner as described for complex **2**. Pure **4** (yield 60.9%) was obtained as reddish brown crystals by recrystallization from CH_2Cl_2/*n*-hexane. Anal. Calcd. for $C_{22}H_{26}Cl_2N_2Ti$ (437.23): C, 60.43; H, 5.99; N, 6.41. Found: C, 60.20; H, 5.90; N, 6.48. ^{1}H NMR ($CDCl_3$, 300 MHz, 298 K): δ 7.93 (d, J = 5.5 Hz, 1H, Py*H*), 7.41−7.33 (m, 3H, Ph*H*), 7.18 (d, J = 8.1 Hz, 1H, Py*H*), 6.54−6.48 (m, 1H, Py*H*), 6.36(d, J = 8.6 Hz, 1H, Py*H*),2.41 (s, 3H, PhCH_3), 2.24 (s, 15H, CpCH_3) ppm. ^{13}C NMR ($CDCl_3$, 75 MHz, 298 K): δ 161.7, 144.8, 141.6, 134.0, 133.7, 129.5, 124.1, 112.3, 103.8(Ar*C*, Py*C*), 21.1 (PhCH_3), 14.0 (CpCH_3) ppm.

4.10. General procedure for olefin polymerization

The ethylene and propylene polymerization experiments were carried out as follows: A dry 250 mL steel autoclave with a magnetic stirrer was charged with 60 mL of toluene and Al^{i}Bu$_3$ in toluene (10 mL), thermostated at desired temperature and saturated with olefin monomer (1.0 atm). A precatalyst solution in toluene (5.0 mL) was then added, immediately followed by addition of a $Ph_3CB(C_6F_5)_4$ solution in toluene (5.0 mL). The vessel was pressurized to 5 atm with olefin monomer immediately and the pressure was kept by continuously feeding of olefin monomer. The reaction mixture was stirred at the desired temperature for 5 min. The polymerization was then quenched by injecting acidified methanol [HCl (3 M)/methanol = 1:1], and the polymer was collected by filtration, washed with water and methanol, and dried at 60 °C in vacuo to a constant weight under vacuum.

4.11. Crystal structure determination

Single crystals of complexes **1**, **2**, **4** and **5** suitable for X-ray crystal structural analysis were obtained from CH_2Cl_2/*n*-hexane (v/v = 1~2:10) mixed solvent system. The data were collected with the *ω-2θ* scan mode on a Bruker SMART 1000 CCD diffractometer with graphite-monochromated Mo-Kα radiation (λ = 0.71073 Å). All structures were solved by direct methods [33] and refined by full-matrix least squares on F^2. All non-hydrogen atoms were refined anisotropically, and the hydrogen atoms were introduced in calculated positions with the displacement factors of the host carbon atoms. All calculations were performed using the SHELXTL crystallographic software packages [34]. Details of the crystal data, data collections, and structure refinements are summarized in Table 4. Crystallographic data (excluding structural factors) for the structures reported in this paper have been deposited with the Cambridge Crystallographic Data Centre as supplementary publication no. CCDC-1409164 [**1**], CCDC-1409165 [**2**], CCDC-1409166 [**4**] and CCDC-1409163 [**5**].

Acknowledgment

This work was supported by the National Natural Science Foundation of China (Nos. 51173061, 21274050 and U1462111).

Appendix A. Supplementary data

Supplementary data related to this article can be found at http://dx.doi.org/10.1016/j.jorganchem.2015.12.029.

References

[1] S. Hansjorg, W. Kaminsky, Transition Metals and Organometallics for Catalysts for Olefin Polymerization, Springer, New York, 1988.
[2] N. Giulio, et al., J. Am. Chem. Soc. 79 (1957) 2975–2976.
[3] R.L. Halterman, Chem. Rev. 92 (1992) 965–994.
[4] P.C. Möhring, N.J. Coville, J. Organomet. Chem. 479 (1994) 1–29.
[5] (a) K. Nomura, Dalton Trans. 41 (2009) 8811–8823;
(b) K. Nomura, J. Liu, S. Padmanabhan, B. Kitiyanan, J. Mol, Catal. A Chem. 267 (2007) 1–29;
(c) D.W. Stephan, Organometallics 24 (2005) 2548–2560.
[6] H.H. Brintzinger, D. Fischer, R. Mülhaupt, et al., Angew. Chem. 107 (1995) 1255–1283.
[7] W. Kaminsky, Macromol. Chem. Phys. 197 (1996) 3907–3945.
[8] A.L. McKnight, R.M. Waymouth, Chem. Rev. 98 (1998) 2587–2598.
[9] G.J.P. Britovsek, V.C. Gibson, D.F. Wass, Angew. Chem. Int. Ed. Engl. 38 (1999) 428–447.
[10] (a) K. Nomura, N. Naga, M. Miki, K. Yanagi, A. Imai, Organometallics 17 (1998) 2152–2154;
(b) K. Nomura, N. Naga, M. Miki, K. Yanagi, Macromolecules 31 (1998) 7588–7597;
(c) K. Nomura, T. Komatsu, Y. Imanishi, J. Mol. Catal. A Chem. 152 (2000) 249–252;
(d) K. Nomura, T. Komatsu, Y. Imanishi, Macromolecules 33 (2000) 8122–8124.
[11] (a) K. Nomura, K. Fujii, Macromolecules 36 (2003) 2633–2641;
(b) P.J. Sinnema, T.P. Spaniol, J. Okuda, J. Organomet. Chem. 598 (2000) 179–181.
[12] K. Nomura, K. Fujii, Organometallics 21 (2002) 3042–3049.
[13] K. Liu, Q. Wu, W. Gao, Y. Mu, L. Ye, Eur. J. Inorg. Chem. 12 (2011) 1901–1909.
[14] L. Rocchigiani, V. Busico, A. Pastore, G. Talarico, A. Macchioni, Angew. Chem. Int. Ed. 53 (2014) 2157–2161.
[15] (a) I. Haas, T. Dietel, K. Press, et al., Chem. A Eur. J. 19 (2013) 14254–14262;
(b) H. Fuhrmann, S. Brenner, P. Arndt, et al., Inorg. Chem. 35 (1996) 6742–6745;
(c) R. Kempe, P. Arndt, Inorg. Chem. 35 (1996) 2644–2649;
(d) M. Oberthur, G. Hillebrand, P. Arndt, R. Kempe, Chem. Ber. 130 (1997) 789–794;
(f) Awal Noor, Dissertation, University of Bayreuth, 2008.
[16] X.-E. Duan, S.-F. Yuan, H.-B. Tong, S.-D. Bai, X.-H. Wei, D.-S. Liu, Dalton Trans. 41 (2012) 9460–9467.
[17] (a) G. Hillebrand, A. Spannenberg, P. Arndt, R. Kempe, Organometallics 16 (1997) 5585–5588;
(b) A. Spannenberg, A. Tillack, P. Arndt, R. Kirmse, R. Kempe, Polyhedron 17 (1998) 845–850;
(d) C. Jones, P.C. Junk, S.G. Leary, N.A. Smithies, Inorg. Chem. Commun. 6 (2003) 1126–1128.
[18] E. Smolensky, M. Kapon, J.D. Woollins, M.S. Eisen, Organometallics 24 (2005) 3255–3265.
[19] (a) C. Jones, P.C. Junk, S.G. Leary, N.A. Smithies, Inorg. Chem. Commun. 6 (2003) 1126–1128;
(b) R. Fandos, C. Hernandez, A. Otero, A. Rodriguez, M.J. Ruiz, J. Organomet. Chem. 690 (2005) 4828–4834.
[20] (a) V. Bertolasi, R. Boaretto, M.R. Chierotti, R. Gobetto, S. Sostero, Dalton Trans. (2007) 5179–5189;
(b) H. Shen, H.-S. Chan, Z. Xie, Organometallics 41 (2007) 2694–2704;
(c) M.L. Cole, P.C. Junk, New J. Chem. 27 (2003) 1032–1037.
[21] S. Pedrosa, F. Vidal, L.M. Lee, et al., Dalton Trans. 44 (2015) 11119–11128.
[22] I. Haas, W.P. Kretschmer, R. Kempe, Organometallics 30 (2011) 4854–4861.
[23] (a) J. Sabimannshausen, M. Bochmann, J. Rösch, D. Lilge, J. Organomet. Chem. 548 (1997) 23–28;
(b) L. Resconi, R.L. Jones, A.L. Rheingold, G.P.A. Yap, Organometallics 15 (1996) 998–1005;
(c) Y.X. Chen, M.D. Rausch, J.C.W. Chien, Macromolecules 28 (1995) 5399–5404.
[24] B.Y. Lee, H.Y. Kwon, S.Y. Lee, S.J. Na, S. Han, H. Yun, H. Lee, Y.-W. Park, J. Am. Chem. Soc. 127 (2005) 3031–3037.
[25] L. Pauling, The Nature of the Chemical Bond, third ed., Cornell University Press, Ithaca, NY, 1960.
[26] L.A. Koterwas, J.C. Fettinger, L.A. Sita, Organometallics 18 (1999) 4183–4190.
[27] (a) Y.-X. Chen, P.-F. Fu, C.L. Stern, T.J. Marks, Organometallics 16 (1997) 5958–5963;
(b) Y.X. Chen, T.J. Marks, Organometallics 16 (1997) 3649–3657.
[28] (a) X. Tao, Q. Wu, H. Huo, W. Gao, Y. Mu, Organometallics 32 (2013) 4185–4191;
(b) X. Tao, W. Gao, H. Huo, Y. Mu, Organometallics 32 (2013) 1287–1294.
[29] (a) F. Zhang, Y. Mu, L. Zhao, Y. Zhang, W. Bu, C. Chen, H. Zhai, H.J. Hong, Organomet. Chem. 613 (2000) 68–76;
(b) F. Zhang, Y. Mu, J. Wang, Z. Shi, W. Bu, S. Hu, Y. Zhang, S. Feng, Polyhedron 19 (2000) 1941–1947.
[30] J.C. Randall, J. Macromol, Sci. Rev. Macromol. Chem. Phys. C29 (1989) 201–317.
[31] (a) M. Björgvinssson, S. Halldorssson, I. Amason, J. Magull, D. Fenske, J. Organomet. Chem. 544 (1997) 207–215;
(b) G.H. Llinas, M. Mena, F. Palacios, P. Royo, R. Serrano, J. Organomet. Chem. 340 (1988) 37–40.
[32] (a) A.G. Massey, A.J. Park, J. Organomet. Chem. 2 (1964) 245–250;
(b) A.G. Massey, A.J. Park, J. Organomet. Chem. 5 (1966) 218–225;
(c) J.C.W. Chien, W.M. Tsai, M.D. Rausch, J. Am. Chem. Soc. 113 (1991) 8570–8571.
[33] G.M. Sheldrick, SHELXTL, Version 5.1, Siemens Industrial Automation, Inc., 1997.
[34] SMART and SAINT Software Packages, Siemens Analytical X-ray instruments, Inc., Madison, WI, 1996.